

Structure of Copper(II)–Histidine Based Complexes in Frozen Aqueous Solutions As Determined from High-Field Pulsed Electron Nuclear Double Resonance

Palanichamy Manikandan, Boris Epel, and Daniella Goldfarb*

Department of Chemical Physics, Weizmann Institute of Science, Rehovot-76100, Israel

Received October 16, 2000

W-band (95 GHz) pulsed EPR and electron–nuclear double resonance (ENDOR) spectroscopic techniques were used to determine the hyperfine couplings of different protons of Cu(II)–histidine complexes in frozen solutions. The results were then used to obtain the coordination mode of the tridentate histidine molecule and to serve as a reference for Cu(II)–histidine complexation in other, more complex systems. Cu(II) complexes with L-histidine and DL-histidine- α - d_2 were prepared in H₂O and in D₂O, and orientation-selective W-band ¹H and ²H pulsed ENDOR spectra of these complexes were recorded at 4.5 K. These measurements lead to the unambiguous assignment of the signals of the H _{α} , H _{β} , imidazole H _{ϵ} , and the exchangeable amino, H_{am}, protons. The ¹⁴N superhyperfine splitting observed in the X-band EPR spectrum and the presence of only one type of H _{α} and H _{β} protons in the W-band ENDOR spectra show that the complex is a symmetric bis complex. Its g_{||} is along the molecular symmetry axis, perpendicular to the equatorial plane that consists of four coordinated nitrogens in histamine-like coordinations (NNNN). Simulations of orientation-selective ENDOR spectra provided the principal components of the protons' hyperfine interaction and the orientation of their principal axes with respect to g_{||}. From the anisotropic part of the hyperfine interaction of H _{α} and H _{β} and applying the point-dipole approximation, a structural model was derived. An unexpectedly large isotropic hyperfine coupling, 10.9 MHz, was found for H _{α} . In contrast, H _{α} of the Cu(II)–1-methyl-histidine complex, where only the amino nitrogen is coordinated, showed a much smaller coupling. Thus, the hyperfine coupling of H _{α} can serve as a signature for a histamine coordination where both the amino and imino nitrogens of the same molecule bind to the Cu(II), forming a six-membered chelating ring. Unlike H _{α} the hyperfine coupling of H _{ϵ} is not as sensitive to the presence of a coordinated amino nitrogen of the same histidine molecule.

Introduction

Copper–histidine coordination is highly abundant in biological systems. Histidine residues serve as ligands in most of the copper enzymes and proteins and play a role in the process of copper transport in biological systems.¹ Recently, copper–histidine complexes were also identified as physiologically significant medicines in the treatment of Menkes and Wilson diseases.² Inspired by the catalytic activity of type 2 Cu(II) centers in copper oxidases,³ Cu(II)–histidine complexes were encapsulated in zeolite Y and were found to catalyze the oxidation of alcohols, alkanes, and alkenes at mild temperatures.⁴ There are three potential coordination sites in the histidine molecule: the amino (N_{am}) nitrogen, the imidazole imido (N _{ϵ} or N _{δ}) nitrogen, and the carboxylate oxygen. The mode of coordination, however, strongly depends on the solution pH, the composition, and the complex environment. This variability has led to numerous studies devoted to the determination of the structure of Cu(II)–histidine complexes in a variety of systems.^{5–9} In proteins the situation is simpler because the amino and the carboxylate groups are unavailable as they are involved

in the creation of the peptide bond, thus leaving only one of the imidazole nitrogens (N _{ϵ} or N _{δ}) as a potential coordination site.

Because of the importance of Cu(II)–histidine based complexes, the coordination geometry of the Cu(II) has been investigated in variety of model systems, such as doped crystals, frozen solutions, and zeolites, by X-ray diffraction, NMR, EPR, and diffuse reflectance spectroscopies.^{4–8,10,11} For example, the crystal structure of Cu(II) doped in L-histidine·HCl·H₂O reveals that the Cu(II) ion is coordinated to amine and imino nitrogens, and a carboxylate oxygen from three different histidine molecules, along with two chloride ions.⁷ This structure is different from that of Cu(II) doped in a Cd(histidinato) complex in the solid state¹² where it was proposed that the Cu(II) coordinates to amine and imino nitrogens, and a carboxylate oxygen of one histidine molecule, and to a carboxyl oxygen of a neighboring histidine molecule. In aqueous solutions, Cu(II)–histidine complexes assume various structures depending on the pH value

- (1) Gray, H. B.; Solomon, E. I. In *Copper Proteins*; Spiro, T. G., Ed.; Metal Ions in Biology 3; Wiley: New York, 1981.
- (2) Sarkar, B. *Chem. Rev.* **1999**, *99*, 2535–2544.
- (3) Lontie, R. In *Copper Proteins and Copper Enzymes*; CRC Press: Boca Raton, FL, 1984; Vols. 1–3.
- (4) Weckhuysen, B. M.; Vertberckmoes, F. L.; Schoonheydt, R. A. *J. Phys. Chem.* **1996**, *100*, 9456–9461.
- (5) Sigel, H.; McCormick, D. B. *J. Am. Chem. Soc.* **1971**, *93*, 2041–2044.

- (6) Basosi, R.; Valensin, G.; Gaggeli, E.; Froncisz, W.; Pasenkiewicz-Gierula, M.; Antholine, W. A.; Hyde, J. S. *Inorg. Chem.* **1986**, *25*, 3006–3010.
- (7) McDowell, C. A.; Naito, A.; Sastry, D. L.; Cui, Y. U.; Sha, K.; Yu, S. X. *J. Mol. Struct.* **1989**, *195*, 361–381.
- (8) Colaneri, M. J.; Peisach, J. *J. Am. Chem. Soc.* **1992**, *114*, 5335–5341.
- (9) Weckhuysen, B. M.; Vertberckmoes, A. A.; Vannijvel, I. P.; Pelgrims, J. A.; Buskens, P. L.; Jacobs, P.; Schoonheydt, R. A. *Angew. Chem., Int. Ed. Engl.* **1995**, *34*, 2652–2654.
- (10) Kruck, T. B. A.; Sarkar, B. *Can. J. Chem.* **1973**, *51*, 3563–3571.
- (11) Valensin, G.; Basosi, R.; Antholine, W. E.; Gaggeli, E. *J. Inorg. Biochem.* **1985**, *23*, 125–130.
- (12) Colaneri, M. J.; Peisach, J. *J. Am. Chem. Soc.* **1995**, *117*, 6308–6315.

and both mono- and bis-histidine complexes were identified.^{5,13–15} Nevertheless, studies based on different spectroscopic techniques vary in their conclusions with respect to the prevailing structure even under the same experimental conditions. For example, at physiological pH (=7.3), Romanelli and Basosi¹⁶ proposed from electron-spin echo modulation (ESEEM) studies that the Cu(II)–histidine complex has two histamine-like coordinations in the equatorial plane and two solvent molecules at the axial positions. In contrast, NMR studies of this complex indicated a mixture of two complexes: one with two histamine-like coordinations and another with one histamine and one glycine-like coordinations.¹¹ Similarly, Goodman et al. and Basosi et al. support the presence of mixed complexes in the solutions but with different ratios.^{6,14,15}

In principle, EPR measurements combined with electron nuclear double resonance (ENDOR) experiments can provide detailed information concerning the first, second, and even the third coordination sphere of the Cu(II)–histidine complex by following the ¹⁴N and ¹H signals. The complete assignment of the ¹H signals of Cu(II)–histidine in aqueous solution has not been reported so far due to the problem of overlapping ¹⁴N and ¹H signals at X-band frequencies.¹⁷ With the advent of high-frequency/high-field ENDOR spectroscopy these problems are overcome because the signals of different types of nuclei are well separated because of their larger nuclear Zeeman energy.^{18–21} In this work we present an orientation-selective^{22,23} W-band (94.9 GHz) pulsed ENDOR investigation aimed at the assignment of the ¹H ENDOR signals and the determination of the structure of the Cu(II)–bis-histidine complex at pH = 7.3. For this purpose, in addition to normal histidine, a histidine deuterated at the α and β positions and a histidine methylated at the N_ε position were used. In addition, the complexes were prepared in H₂O and D₂O solutions to identify the exchangeable protons, and both ¹H and ²H spectra were recorded. This allowed the unambiguous assignment of the various ENDOR signals to specific protons in the histidine molecule. By measurement of orientation-selective ENDOR spectra, which were further analyzed by computer simulations, it was also possible to determine the magnitude and orientation of the ¹H hyperfine interaction. For some of the protons these were further interpreted in terms of the orientation of the ¹H–Cu(II) vector with respect to the molecular symmetry axis, providing the conformation of the histidine ligands in the complex. These results can serve as a basis for future studies requiring the structure of Cu(II)–histidine complexes in other systems such as complexes encapsulated in zeolite cages.²⁴

Experimental Section

Sample Preparation. The Cu(II)–histidine complexes were prepared according to reported procedures.⁵ A typical preparation procedure involves mixing, in a molar ratio of 1:5, anhydrous CuCl₂ and L-histidine·HCl·H₂O (Merck) or DL-histidine- α -d, β -d₂ (CDN Isotopes) or 1-methyl-L-histidine (ICN Biochemicals Inc.) in H₂O or D₂O (Cambridge Isotope Laboratories, Inc.). The solution was stirred for an hour at room temperature. The pH/pD of the solution was adjusted to 7.3 using 0.1 N NaOH/NaOD (ISOTEC, Inc.) and/or dilute H₂SO₄/D₂SO₄ (Sigma Co.) solutions. Glycerol or glycerol-d₃ (Cambridge Isotope Laboratories, Inc.) were used to produce a good glass upon freezing. The [Cu(imidazole)₄]Cl₂ complex was prepared as reported earlier.²⁵ The concentrations of all the Cu(II) complexes were 2 mM. All the chemicals were used without further purifications.

Spectroscopic Measurements. Continuous wave (CW) X-band EPR spectra were measured at ~9.16 GHz and ~150 K, using a Varian E-12 EPR spectrometer. W-band pulsed EPR and ENDOR measurements were carried out at 94.9 GHz and 4.5 K using a home-built spectrometer described elsewhere.²⁶ Field-sweep (FS) echo-detected (ED) EPR spectra were recorded using the two-pulse echo sequence ($\pi/2$ - τ - π - τ -echo) where the echo intensity was registered as a function of the magnetic field. Typically, microwave (MW) pulse lengths (t_{MW}) of 0.05 and 0.1 μ s were used with $\tau = 0.3 \mu$ s. The magnetic field values were calibrated using the Larmor frequency of the protons, ν_H , as determined by the ENDOR measurements. The ¹H ENDOR spectra were measured using the Davies ENDOR pulse sequence (π - T - $\pi/2$ - τ - π - τ -echo) with an rf pulse applied during the time interval T .²⁷ The Mims ENDOR sequence $\pi/2$ - τ - $\pi/2$ - T - $\pi/2$ - τ -echo with an rf pulse applied during the time T was used for the ²H ENDOR measurements.²⁸ The experimental conditions for the Davies ENDOR spectra were $t_{MW} = 0.2, 0.1, 0.2 \mu$ s, $\tau = 0.5 \mu$ s, $t_{RF} = 25 \mu$ s, and for the Mims ENDOR they were $t_{MW} = 0.1, 0.1, 0.1 \mu$ s, $\tau = 0.25 \mu$ s, $t_{RF} = 40 \mu$ s. The intensity and frequency scales of the ²H spectra were multiplied by -1 and γ^H/γ^D (=6.5144), respectively, to allow a convenient comparison with the ¹H ENDOR spectra. The frequency scale in the ¹H and ²H ENDOR spectra is given with respect to the Larmor frequency, $\nu = \nu_{RF} - \nu_H$.

Spectral Simulations. The ENDOR spectra were simulated using a computer program developed in our group based on the theory presented by Erickson²⁹ for $S = 1/2$ with n interacting nuclei. The spin Hamiltonian used has the form

$$H = \beta \vec{B} \cdot \mathbf{g} \cdot \hat{S} + \sum_{i=1}^n [-g_N \beta_N \vec{B} \cdot \hat{I}_i + \hat{S} \cdot \mathbf{A}_i \cdot \hat{I}_i + \hat{I}_i \cdot \mathbf{Q}_i \cdot \hat{I}_i] \quad (1)$$

where \vec{B} is the external magnetic field and \mathbf{A}_i and \mathbf{Q}_i correspond to the hyperfine and quadrupole tensors, respectively, of nucleus i . Since in this work we simulated only ¹H spectra, the last term in eq 1 can be ignored. \mathbf{A}_i is described by its three principal values, A_{ixx} , A_{iyy} , and A_{izz} , and the Euler angles (α_i , β_i , γ_i) that transform its principal axis system (x'', y'', z'') to that of \mathbf{g} (x', y', z'). In the case of an axial \mathbf{g} tensor, the principal values are g_{\perp} and g_{\parallel} and only two Euler angles are required, β_i and γ_i . The angles θ_0 and ϕ_0 transform the \mathbf{g} tensor from its principal system into the laboratory frame where $Z \parallel \vec{B}$. When the anisotropic hyperfine can be described by the point-dipole approximation, the principal values of \mathbf{A}_i become $A_{ixx} = A_{iyy} = A_{i\perp\perp} = -a_{i\perp} + a_{i\text{iso},i}$ and $A_{izz} = 2a_{i\perp} + a_{i\text{iso},i}$ where $a_{i\perp}$ represents the dipolar part of the interaction,

(13) Sigel, H.; Griesser, R.; McCormick, D. B. *Arch. Biochem. Biophys.* **1960**, *134*, 217–227.

(14) Goodman, B. A.; McPhail, D. B.; Powell, H. K. *J. Chem. Soc., Dalton Trans.* **1981**, 822–827.

(15) Szabó-Plánka, T.; Rockenbauer, A.; Györ, M.; Gaizer, F. *J. Coord. Chem.* **1988**, *17*, 69–83.

(16) Romanelli, M.; Basosi, R. *Chem. Phys. Lett.* **1988**, *143*, 404–408.

(17) Scholl, H.-J.; Huttermann, J. *J. Phys. Chem.* **1992**, *96*, 9684–9691.

(18) Möbius, K. In *Biological Magnetic Resonance*; Berliner, L. J., Reuben, J., Eds.; Plenum Press: New York, 1993; Vol. 13, pp 253–274.

(19) Coremans, J. W. A.; Poluektov, O. G.; Groenen, E. J. J.; Canters, G. W.; Nar, H.; Messerschmidt, A. *J. Am. Chem. Soc.* **1996**, *118*, 12141–12153.

(20) Arieli, D.; Vaughan, D. E. W.; Strohmaier, K. G.; Goldfarb, D. *J. Am. Chem. Soc.* **1999**, *121*, 6028–6032.

(21) Manikandan, P.; Carmieli, R.; Shane, T.; Kalb, A. J.; Goldfarb, D. *J. Am. Chem. Soc.* **1000**, *122*, 3488–3494.

(22) Hurst, G. C.; Henderson, T. A.; Kreilick, R. W. *J. Am. Chem. Soc.* **1985**, *107*, 7294–7299.

(23) Hoffman, B. M.; Martinsen, J.; Venters, R. A. *J. Magn. Reson.* **1984**, *59*, 110–123.

(24) Grommen, R.; Manikandan, P.; Gao, Y.; Shane, T.; Shane, J. J.; Schoonheydt, R. A.; Weckhuysen, B. M.; Goldfarb, D. *J. Am. Chem. Soc.* **2000**, *122*, 11488–11496.

(25) Van Camp, H. L.; Sands, R. H.; Fee, J. A. *J. Chem. Phys.* **1981**, *75*, 2098–2107.

(26) Gromov, I.; Krymov, V.; Manikandan, P.; Arieli, D.; Goldfarb, D. *J. Magn. Reson.* **1999**, *139*, 8–17.

(27) Davies, E. R. *Phys. Lett.* **1974**, *47A*, 1–2.

(28) Mims, W. B. *Proc. R. Soc. London, Ser. A* **1965**, *283*, 452–457.

(29) Erickson, R. *Chem. Phys.* **1996**, *202*, 263–275.

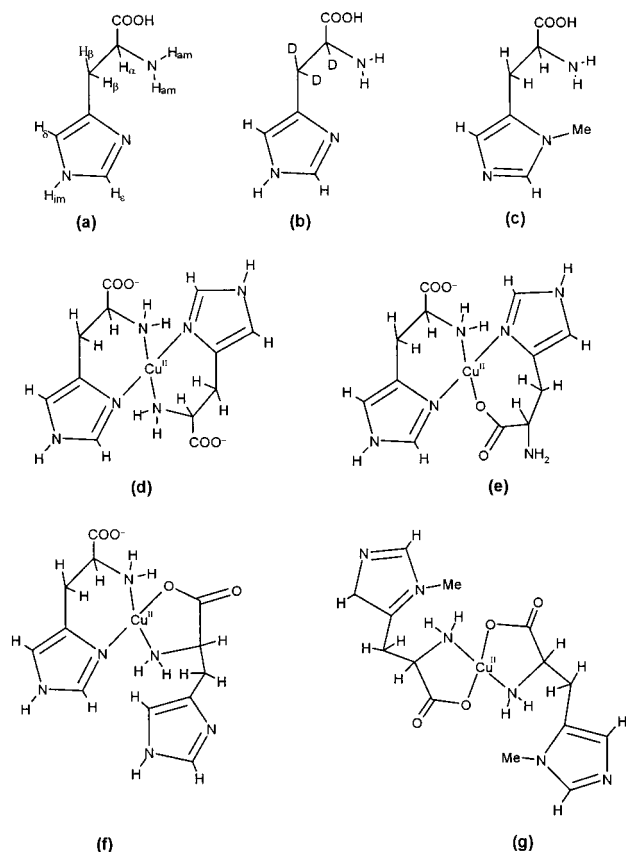


Figure 1. Schematic representations of (a) histidine, (b) histidine- α - d_3 , (c) 1-methyl-histidine, (d) Cu(II)–histidine complex with NNNN coordination, (e) Cu(II)–histidine complex with NNNO coordination and a seven-membered chelating ring, (f) Cu(II)–histidine complex with NNNO coordination and a five-membered chelating ring, (g) Cu(II)–1-methyl-histidine complex with NNOO coordination. Solvent molecules are not drawn in the figure.

$$a_{i\perp} = \frac{\mu_0 g \beta g_N \beta_N}{4\pi r_i^3 h}$$

$a_{i\text{iso},i}$ is the isotropic part, and r_i is the electron-nuclear distance.

Results

Assignment of ENDOR Signals. Schematic representations of the histidine-based ligands used in this work and possible molecular structures of their Cu(II) complexes are given in Figure 1. The nomenclature used in this work for the various protons is indicated in Figure 1a. The CW X-band EPR spectra of the Cu–(L-histidine)₂ (Cu–His), Cu–(DL-histidine- α - d_3)₂ (Cu–His- d_3), Cu–(1-methyl-histidine)₂ (Cu–MeHis), and Cu(imidazole)₄ (Cu–Imid) in a frozen aqueous solution (pH = 7.3) are shown in Figure 2, and the EPR parameters are summarized in Table 1. The spectra of the Cu(II) complexes with L-histidine and DL-histidine are identical, and all the complexes exhibit a powder pattern characteristic of axial symmetry. Only the spectrum of Cu–Imid (trace iv, Figure 2a) exhibits clear ¹⁴N superhyperfine splittings at the ^{63,65}Cu $m_I = 3/2$ hyperfine component (near g_{\perp}) due to nitrogen coordination. In all other spectra the splittings are either not well resolved or can be barely noticed. In the case of Cu–His- d_3 (trace ii, Figure 2a) it was possible to resolve a nine-line splitting pattern in the second derivative spectrum because of coordination to four nitrogens in the first coordination shell. As expected, the EPR spectrum of Cu–MeHis (trace iii, Figure 2a) is different from that of Cu–His, since the N_{ϵ} coordination is blocked because

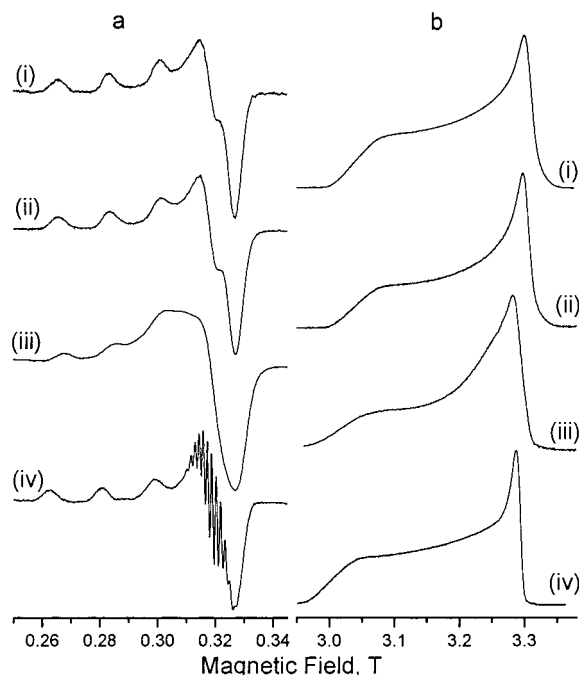


Figure 2. (a) CW X-band EPR spectra (150 K) of (i) Cu–His, (ii) Cu–His- d_3 , (iii) Cu–MeHis, (iv) Cu–Imid complexes in H₂O/glycerol. (b) Corresponding W-band FS-ED EPR spectra measured at 4.5 K.

Table 1. EPR Parameters of the Cu(II)–Histidine Complexes^a

complex	g_{\parallel} (± 0.005)	g_{\perp} (± 0.0005)	$A_{\parallel}(\text{Cu})$ (± 0.1), mT	$A_{\perp}(\text{N})$ (± 0.05), mT
Cu–His in D ₂ O	2.24	2.058	17.8	1.4
Cu–His- d_3 in D ₂ O	2.24	2.058	17.8	1.4
Cu–MeHis in D ₂ O	2.23	2.063	17.5	
Cu–Imid in H ₂ O	2.26	2.062	18.3	1.5

^a g_{\parallel} was determined from the CW X-band EPR spectra at 150 K, whereas g_{\perp} was obtained from W-band FS-ED EPR at 4.5 K.

of methylation. The W-band FS-ED EPR spectra of these complexes are depicted in Figure 2b. All spectra exhibit a powder pattern characteristic of an axial tensor where the ^{63,65}-Cu hyperfine splitting is unresolved. The g values obtained are listed in Table 1.

The ¹H ENDOR spectrum of Cu–His in H₂O, recorded at the g_{\perp} position, is shown in Figure 3a. The spectrum is rather complicated and consists of contributions from a number of protons. Assuming that in the Cu–His complexes the Cu(II) coordinates to two symmetrically situated histidine ligands with a histamine-like coordination, the ENDOR spectrum should consist of the following contributions from each histidine: (i) three imidazole protons (H_{δ} , H_{ϵ} , and H_{im}), (ii) one proton at the C_{α} position (H_{α}), (iii) two protons on C_{β} (H_{β}), and (iv) two exchangeable protons on the amino nitrogen, H_{am} . In addition, water protons (H_{w}), from weak axial coordination, cannot be excluded. Hence, the assignment of the signals to the various protons is not straightforward. The signals of the exchangeable protons can be identified by comparing the spectra of Cu–His prepared in H₂O and D₂O solutions. The ²H and ¹H ENDOR spectra of Cu–His in D₂O (traces b and c of Figure 3) consist of signals of only exchangeable and nonexchangeable protons, respectively. The broad signals appearing at about $\pm 3.4(0.1)$ and $\pm 6.5(0.2)$ MHz in the ²H spectrum are missing in the ¹H ENDOR spectrum and are therefore assigned to H_{am} . The number in brackets represents the uncertainty of the measurement. The signals at $\pm 2.2(0.1)$ MHz and $\pm 1.1(0.05)$ MHz in the ²H ENDOR spectrum (Figure 3b) are assigned to H_{w} because

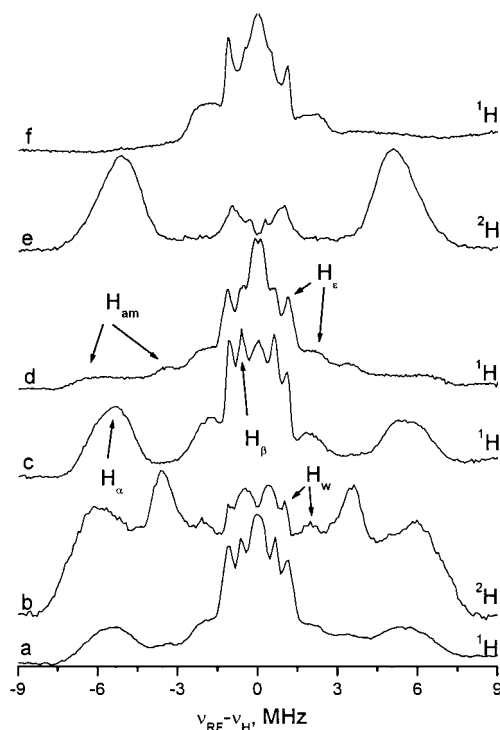


Figure 3. ENDOR spectra of Cu(II)-histidine complexes measured at the g_{\perp} position (4.5 K): (a) ^1H ENDOR spectrum of the Cu-His complex in H_2O ; (b) ^2H ENDOR and (c) ^1H ENDOR spectra of the Cu-His complex in D_2O ; (d) ^1H ENDOR and (e) ^2H ENDOR spectra of Cu-His- d_3 complex in H_2O ; (f) ^1H ENDOR spectrum of the Cu-His- d_3 complex in D_2O . The ^2H ENDOR spectra are plotted in the ^1H frequency scale.

the coupling of a proton on an axial water ligand is expected to be significantly smaller than that of H_{am} .

The ^1H ENDOR spectrum of Cu-His in D_2O (Figure 3c) consists of a relatively broad doublet at $\pm 5.2(0.2)$ MHz and two powder-like patterns below ± 3 MHz, corresponding to the nonexchangeable protons. To distinguish the imidazole protons (H_{δ} and H_{ϵ}) from H_{α} and H_{β} , ENDOR measurements were carried out on Cu-His- d_3 in H_2O and D_2O solutions. The ^1H and ^2H ENDOR spectra of Cu-His- d_3 in H_2O are shown in spectra d and e of Figure 3, respectively. The ^1H spectrum exhibits signals only from H_{am} , H_w , H_{δ} and H_{ϵ} ; hence, a comparison of traces a and d in Figure 3 leads to the following assignment: the $\pm 5.2(0.2)$ MHz doublet is due to H_{α} , H_{β} appears at $\pm 0.62(0.03)$ MHz, and the signals corresponding to the distant imidazole protons (H_{δ}) appear at $\pm 0.50(0.01)$ MHz. The assignment of the H_{α} and H_{β} signals is also confirmed by the ^2H ENDOR spectrum of Cu-His- d_3 in H_2O (Figure 3e). The H_{am} spectrum with singularities appearing at $\pm 3.4(0.1)$ and $\pm 6.6(0.2)$ MHz (Figure 3d) agrees well with the ^2H ENDOR spectrum of Cu-His in D_2O (Figure 3b). Fortunately, the relatively small ^2H quadrupole coupling introduces only some additional broadening, thus allowing line positions to match just by multiplying the ^2H frequency scale by $\gamma^{\text{H}}/\gamma^{\text{D}}$ ($=6.5144$). The ^1H ENDOR spectrum of Cu-His- d_3 in D_2O (Figure 3f) exhibits only signals of H_{δ} and H_{ϵ} , and the powder pattern with features at $\pm 1.09(0.02)$ and $\pm 2.0(0.3)$ MHz is assigned to H_{ϵ} . The ^2H ENDOR spectrum (not shown) of this sample is more complex and consists of the overlapping signals of H_{α} , H_{β} , and deuterons corresponding to the exchangeable protons. In all of the above spectra, signals very close to the Larmor frequency are due to the solvent and far away protons, and they will not be discussed any further. The assignments of ENDOR signals of the various protons are summarized in Table 2 and labeled in Figure 3.

Table 2. Assignment of the ENDOR Signals of the Various Protons in the Cu(II)-Histidine Complexes As Measured from Cu-L-Histidine and Cu-DL-Histidine- α - d_3 - β - d_2 Complexes in H_2O /Glycerol and D_2O /Glycerol- d_3 Measured near the g_{\perp} Position

proton	position of signals, ^a MHz	proton	position of signals, ^a MHz
H_{α}	$\pm 5.20(0.20)$	H_{ϵ}	$\pm 1.09(0.02), \pm 2.0(0.3)$
H_{β}	$\pm 0.62(0.03)$	H_{am}	$\pm 3.40(0.10), \pm 6.5(0.2)$
H_{δ}	$\pm 0.50(0.01)$	H_w	$\pm 2.2(0.1), \pm 1.1(0.05)$

^a The number in parentheses indicate the uncertainty.

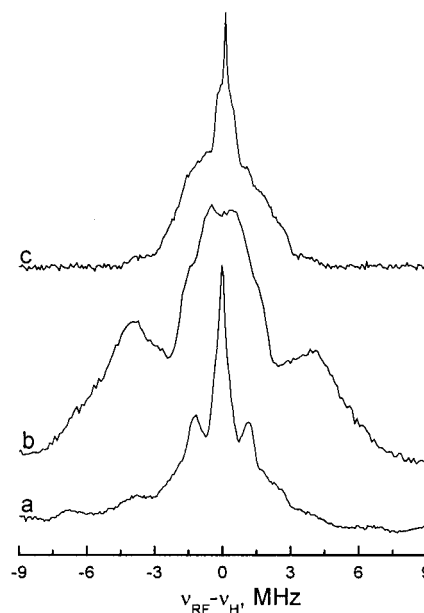


Figure 4. ^1H ENDOR spectrum of Cu-MeHis in H_2O , (b) ^1H ENDOR and (c) ^2H ENDOR spectra of Cu-MeHis in D_2O measured at g_{\perp} and 4.5 K. The ^2H ENDOR spectrum is plotted in the ^1H frequency scale.

To evaluate the sensitivity of the hyperfine coupling constants of various protons of histidine to the coordination mode of the Cu(II), the Cu-MeHis complex was prepared in H_2O and D_2O . Because of the methylation at the N_{ϵ} position, the imidazole nitrogen is no longer a coordination site in this complex. As a result, a complex with two MeHis ligands coordinated in a glycine-like mode at the equatorial positions, or with four MeHis coordinated via amine nitrogens, is expected. The g and $A(\text{Cu})$ values of this complex are very close to that of Cu-His (see Table 1), thus favoring the four-amine coordination geometry. The ^1H and ^2H ENDOR spectra measured at the g_{\perp} position are shown in Figure 4. The absence of the strong signals at $\pm 5.2(0.2)$ MHz assigned earlier to H_{α} is clear. The only nonexchangeable protons that contribute to the ^1H ENDOR spectrum of Cu-MeHis in D_2O (Figure 4c) are H_{α} and H_{β} . The signals of these two protons do not exceed ± 3.7 MHz, and most probably the features giving the larger doublets are due to H_{α} .

Orientation-Selective ENDOR Measurements. Having identified the signals of the various protons/deuterons, we proceeded with orientation-selective experiments designed to provide the principal components of the hyperfine interaction and the relative orientation of its principal axes with respect to the direction of g_{\parallel} . These, in turn, yield the conformation of the ligands in the metal complex. We started with the ^1H ENDOR signals of H_{α} in the spectra of Cu-His in D_2O , shown in Figure 5a, where they are well-resolved. As the magnetic field approaches g_{\parallel} , the spectra become more and more asymmetric. This is not due to instrumental problems or baseline drift but originates from partial saturation of the NMR transi-

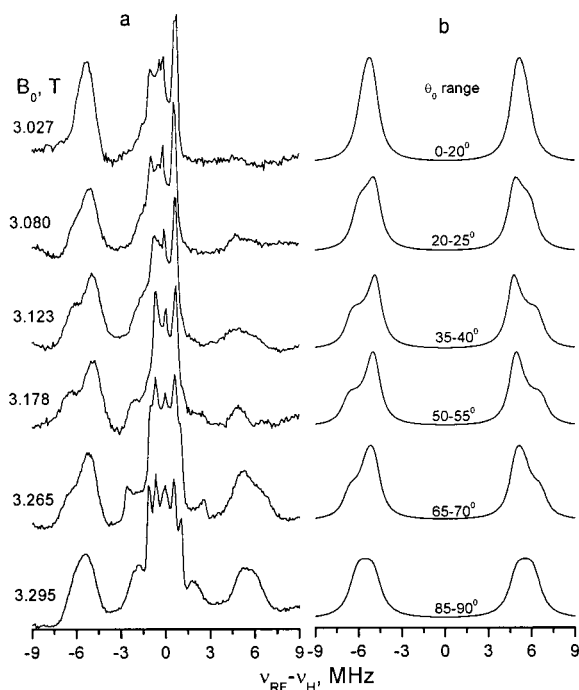


Figure 5. (a) Field-dependent ^1H ENDOR spectra (experimental) of the Cu–His complex in D_2O at 4.5 K. (b) Simulated ^1H ENDOR spectra of H_α . The θ_0 range used for the simulations and the corresponding fields are given near each spectrum. The parameters used for the simulations are given in Table 3.

Table 3. Principal Components of the Hyperfine Tensor and the Euler Angles Relating Its Orientation to the \mathbf{g} Tensor As Obtained from the Simulation of the Orientation-Selective ENDOR Spectra

protons	A_{xx} , MHz	A_{yy} , MHz	A_{zz} , MHz	α , deg	β , deg	γ , deg
H_α	± 9.6	± 9.6	± 13.5	0	60	0
H_ϵ	∓ 1.0	∓ 2.4	± 5.4	0	70	0
H_{am}^1	± 6.0	± 7.0	± 14.0	0	20	90
H_{am}^2	± 6.0	± 10.0	± 14.0	0	84	90

tions.³⁰ The line shape and field dependence of the H_α signals were simulated, as shown in Figure 5b, and the simulation parameters are listed in Table 3. The integration range used for ϕ_0 was $0-180^\circ$ for all spectra and that for θ_0 is listed in the figure. H_α exhibits an axially symmetric hyperfine interaction ($A_\perp = 9.6$ MHz and $A_\parallel = 13.5$ MHz) with a relatively large isotropic hyperfine coupling and a small anisotropic component. The latter corresponds to a Cu– H_α distance of 4.0 Å assuming that the point-dipole approximation is valid. The simulations also yield $\beta = 60^\circ$, where β is the angle between the direction of the major principal axis of the hyperfine direction and the g_\parallel axis.

The hyperfine parameters of H_{am} were obtained from orientation-selective ^2H ENDOR spectra of Cu–His in D_2O (Figure 6) and ^1H ENDOR spectra of Cu–His- d_3 in H_2O (Figure 7a). The ^2H ENDOR spectra consist primarily of H_{am} signals, which exhibit large hyperfine couplings because the amine protons are close to the Cu(II) (see Discussion), and of the imino proton of the imidazole ring (H_{im}), which is expected to have a considerably smaller hyperfine coupling. In addition, the presence of weakly coupled protons from an axial water ligand cannot be excluded at this point. Accordingly, the broad but intense ^2H ENDOR signals appearing at $\pm 3.4(0.1)$ and $\pm 6.5(0.2)$ MHz in the spectrum recorded at g_\perp (3.295 T) (Figure 6) are assigned

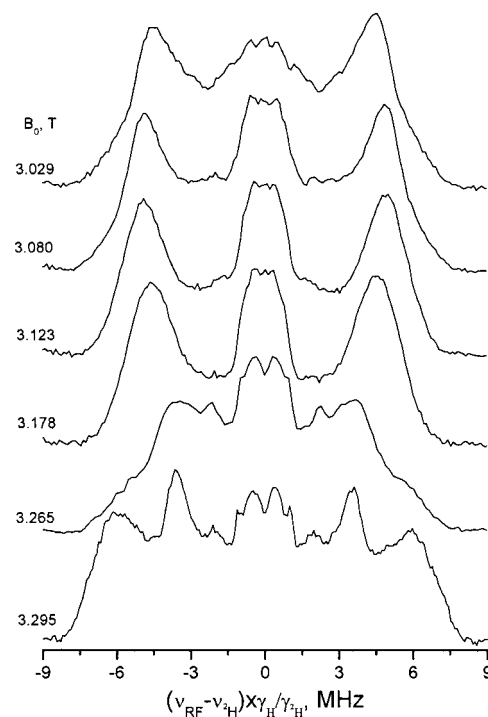


Figure 6. Field-dependent ^2H ENDOR spectra (in ^1H frequency scale) of the Cu–His complex in D_2O , measured at 4.5 K.

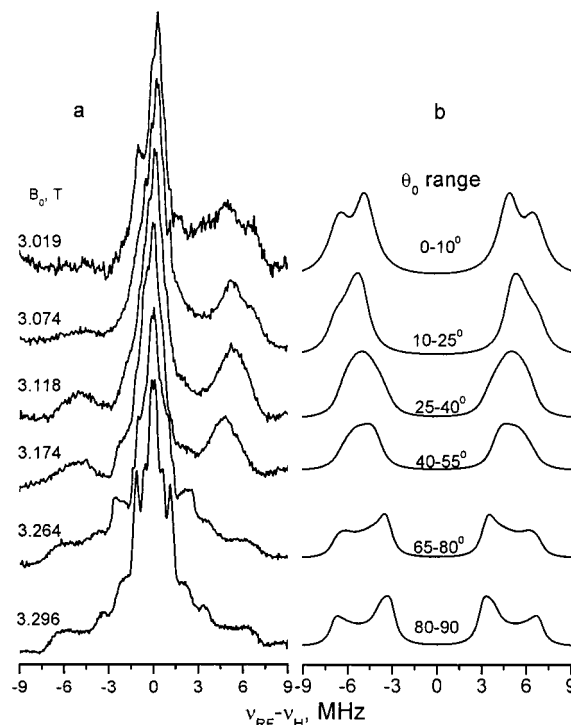


Figure 7. (a) Experimental ^1H ENDOR spectra of Cu–His- d_3 in H_2O measured at different fields and 4.5 K. (b) Corresponding computer simulations of the H_{am} protons. The θ_0 range is noted near the spectra, and the parameters used for the simulations are given in Table 3.

to H_{am} . These ^2H ENDOR singularities merge as the magnetic field decreases and then spread apart again at g_\parallel . While the ^2H ENDOR signals allowed us to identify the H_{am} singularities and their field dependence, their spectral resolution is relatively poor because of quadrupolar splitting. A better resolution of the H_{am} signals is obtained from the ^1H ENDOR spectra of Cu–His- d_3 in H_2O as shown in Figure 7a. The spectral features observed could not be reproduced by a single nucleus or two different

(30) Epel, B.; Pöpl, A.; Vega, S.; Goldfarb, D. *J. Magn. Reson.*, in press.

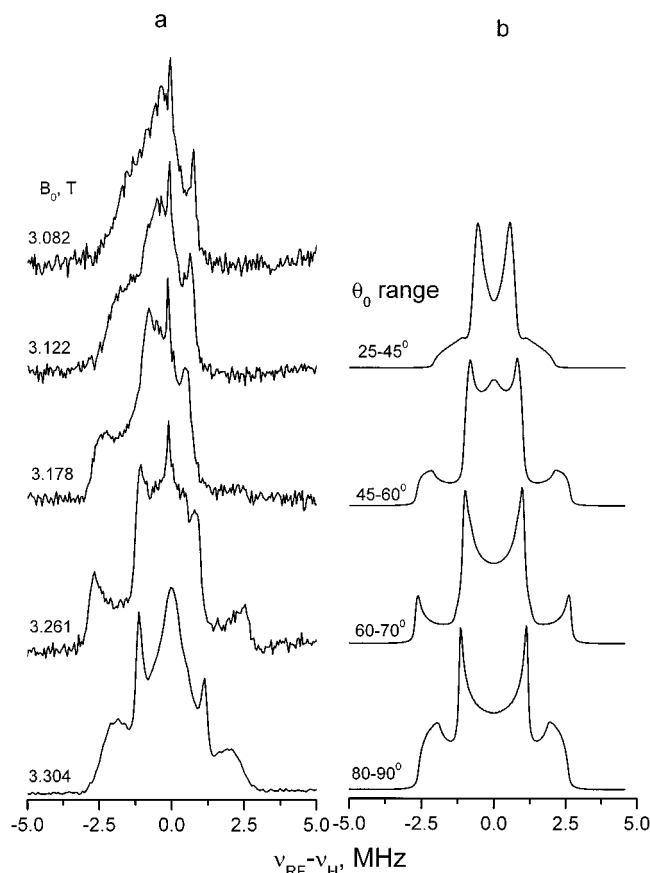


Figure 8. Experimental ^1H ENDOR spectra of the Cu–His- d_3 complex in D_2O measured at different fields (4.5 K). (b) Computer simulations of the ENDOR spectra of H_ϵ .

nuclei with axially symmetric tensors. Hence, the ^1H ENDOR signals of H_{am} were simulated using two nuclei with different nonaxial hyperfine interactions. The simulated spectra of H_{am} are given in Figure 7b. The hyperfine coupling parameters and the Euler angles used for the simulation are listed in Table 3.

The ^1H ENDOR spectra of Cu–His- d_3 in D_2O is relatively simple and consist of the signals of imidazole protons (H_δ , H_ϵ) only. Orientation-dependent ^1H ENDOR spectra are presented in Figure 8a. The quality of the spectra recorded at fields close to g_{\parallel} fields is poor because of low S/N and the large asymmetry; nevertheless, it was possible to simulate the H_ϵ features in the range 3.3036–3.1775 T as shown in Figure 8b. The spectra were simulated with a nonaxial hyperfine tensor as listed in Table 3.

Finally, for the sake of reference and completeness, orientation-selective ^1H ENDOR measurements were also carried out on Cu–Imid in H_2O , and ENDOR spectra at a few selected magnetic fields are given in Figure 9. X-band ENDOR measurements of this system, showing ^{15}N and ^1H signals, were reported.²⁵ In addition X-band ^1H ENDOR spectra recorded at g_{\perp} and g_{\parallel} positions were simulated by using the crystal structure parameters.¹⁷ Here we present the ^1H W-band ENDOR spectra of Cu–Imid in H_2O to show that in the histidine complex the hyperfine coupling of the imidazole proton, H_ϵ , is considerably less susceptible than H_α to the coordination mode.

Discussion

The resolved ^{14}N superhyperfine splittings at the $m_I = 3/2$ $^{63,65}\text{Cu}$ hyperfine component of the CW X-band EPR spectra show that the Cu(II)–histidine complex in a frozen aqueous solution (pH = 7.3) must be a bis complex. Further details about

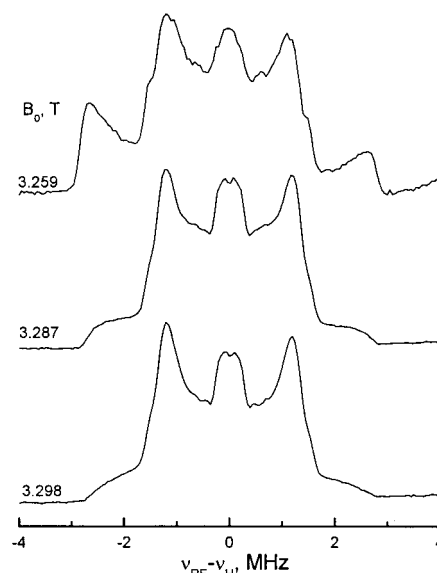


Figure 9. ^1H ENDOR spectra of Cu(imidazole) $_4$ complex in H_2O measured at different magnetic fields.

the specific coordination mode and conformation of the ligands were obtained from orientation-selective W-band ^1H and ^2H ENDOR measurements. In these measurements we concentrated on the ENDOR signals of three types of protons: H_{am} , H_ϵ , and H_α . The first provides evidence for the coordination of the amino nitrogen, N_{am} , whereas the second reports on the imino nitrogen, N_{imid} , coordination. The most significant and useful is the hyperfine coupling of H_α , which was found to be highly sensitive to the coordination mode of the histidine. When both N_{am} and N_{imid} of a particular histidine molecule are coordinated to the Cu(II) ion (histamine coordination), forming a six-membered chelating ring, H_α assumes a large isotropic hyperfine coupling, 10.9 MHz. In contrast, when the coordination is only through one nitrogen, N_{am} , its isotropic hyperfine coupling is significantly smaller (<3 MHz). Accordingly, the hyperfine coupling of H_α can be used as a signature for the coordination mode of Cu(II)–histidine complexes. H_ϵ , on the other hand, is rather insensitive to these structural changes. Only one type of H_α signal was identified in the ENDOR spectra of all the Cu–His complexes investigated (D,L natural abundance and deuterated in the α and β positions). Therefore, we conclude that the complex present in frozen aqueous solutions at pH = 7.3, prepared with excess histidine, is Cu(II)(histidine) $_2$, where N_{am} and N_{imid} of both histidines are coordinated at the equatorial positions, forming two chelating rings, thus confirming the NNNN equatorial coordination.⁵

Through computer simulations of the orientation-selective ENDOR signals of H_α , H_ϵ , and H_{am} , the principal components of the hyperfine tensor, and the relative orientation of its z'' axis with respect to the g_{\parallel} direction, z' , given by β , was determined. In principle, if z' and z'' can be associated with easily identified geometrical characteristics of the molecule, then β provides straightforward conformational information. Since we did not detect different ENDOR signals corresponding to the same type of proton in the two histidine ligands, we conclude that the complex is symmetric and the direction of g_{\parallel} is along the molecular symmetry axis normal to the equatorial plane. The anisotropic hyperfine interaction of H_α is axially symmetric and relatively small. It is therefore reasonable to assume that it can be described by the point-dipole approximation where z'' is along the Cu– H_α direction. Consequently, we obtained from the anisotropic hyperfine value a distance of 4.0 Å with $\beta =$

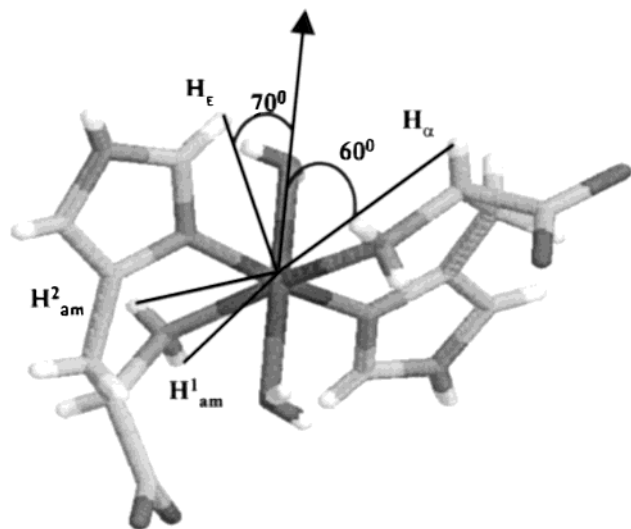


Figure 10. Computer model of the molecular structure of the Cu–His complex (D configuration) determined using geometrical parameters obtained from the ENDOR measurements.

60° . This indicates that H_α is situated above or below the equatorial plane, pointing away from the Cu(II) ion.

A computer model of the complex has been constructed as follows: two histidine molecules (D configuration) were placed in the equatorial positions, and two water molecules were fixed at a rather long Cu–O distance (2.2 \AA) in the axial positions to avoid any other axial coordination. The H_α protons were fixed at 4.0 \AA with $\beta = 60^\circ$ with respect to the normal to the NNNN coordination plane, along the Cu–O (water) axis. The position and geometry of the rest of the molecules were optimized freely using the software Cerius² of MSI.³¹ Thus, the Cu(II) is in an elongated octahedral environment with the four coordinating nitrogens of two histidines in the equatorial plane as shown in Figure 10.

When the point-dipole approximation applies, the correlation between the anisotropic hyperfine and the geometrical parameters of the molecules is straightforward and the structural information is easily extracted. This is not the case when this approximation is not valid, and one has to take into account the spin density on nuclei other than the Cu(II). The ENDOR simulations showed that the hyperfine interaction of H_ϵ and H_{am} protons is nonaxial, indicating that the point-dipole approximation is not appropriate and that therefore the Cu–H distance cannot be readily calculated. Table 4 lists the values of Cu–H and β for these protons as obtained from the model complex discussed above (Figure 10). These distances would have resulted in a_\perp values of $2.4(0.1)$, $4.5(0.1)$, and $5.2(0.4)$ MHz for H_ϵ , $H_{am}(1)$, and $H_{am}(2)$, respectively. The experimental a_\perp

Table 4. Cu–H Distances (\AA) and the Angle β between the Cu–H Vector and the Molecular Symmetry Axis for Various Protons in the Cerius2 Minimized Model of Cu–His^a

proton	Cu–H, \AA	β , deg	a_\perp , ^b MHz
H_α ^c	4.0	60	1.3
H_ϵ	3.26 (0.02)	66 (8)	2.4 (0.1)
H_{am}^1	2.64 (0.02)	85 (5)	4.5 (0.1)
H_{am}^2	2.51 (0.05)	77 (7)	5.2 (0.4)

^a Geometrical parameters for the two histidine ligands were slightly different, and the listed values are the average. The difference is noted in parentheses. ^b Calculated from the Cu–H distance using the point-dipole approximation. ^c Positions of this proton have been fixed according to the experimental results.

value, 2.37 MHz , of H_ϵ (calculated from $(1/6)[2A_{zz} - (A_{yy} + A_{xx})]$) compares reasonably with the geometry of the model. Consequently, we can assume that the direction of z'' is approximately along Cu– H_ϵ and that β can be used to obtain information regarding the conformation. Indeed the β value obtained from the model is 66° , close to the experimental value of 70° . The values calculated for $H_{am}(1)$ and $H_{am}(2)$ deviate significantly from the experimental values because the point-dipole approximation is far from being valid for these protons.

Conclusions

W-band ^1H and ^2H ENDOR spectra of the Cu(II) complexes with L-histidine, DL-histidine- α - d_2 , and 1-methyl-histidine in frozen solutions of H_2O and D_2O ($\text{pH} = 7.3$) enabled us to assign the ENDOR signals of the different protons in the Cu(II)–histidine complex. This information was then used to determine the coordination mode of the complex, which was found to consist of two histidine ligands symmetrically placed in the equatorial positions with NNNN configuration. Orientation-selective ENDOR measurements and their computer simulations gave the magnitude of the principal components of the hyperfine interaction and its orientation with respect to the \mathbf{g} tensor principal axis system. This provided information regarding the conformation of the histidine ligands. The hyperfine coupling of H_α is highly sensitive to the coordination mode. It has a large isotropic hyperfine coupling when both nitrogens of one histidine molecule are coordinated, generating a six-membered chelating ring, and it is significantly smaller when only the amino nitrogen is coordinated. Hence, the hyperfine coupling of H_α can be used as a probe for the mode of coordination of histidine ligands. In contrast, H_ϵ and H_{am} are not very sensitive to the presence of a chelating coordination. These properties of the proton hyperfine couplings are expected to be useful in the investigation of Cu–histidine complexes in a variety of more complex environments such as zeolites.

Acknowledgment. We thank Dr. C. E. Slutter for helpful discussions and suggestions.

(31) Cerius2; Molecular Simulations Inc.: San Diego, CA, 1998.